Short communication

Synthesis of sub-10 nm copper sulphide rods as high-performance anode for long-cycle life Li-ion batteries

Mingjiong Zhou [a], Na Peng [a], Zhen Liu [a], Yun Xi [a], Huiqiu He [a], Yonggao Xia [b, *], Zhaoping Liu [b, **], Shigeto Okada [c]

[a] School of Materials Science and Chemical Engineering, Ningbo University, Fenghua Road 818, Jiangbei District, Ningbo 315211, Zhejiang Province, People's Republic of China
[b] Ningbo Institute of Industrial Technology, Chinese Academy of Science, Ningbo 315201, Zhejiang Province, People's Republic of China
[c] Institute for Materials Chemistry and Engineering, Kyushu University, 6-1 Kasuga-koen, Kasuga 816-8580, Japan

HIGHLIGHTS

- Copper sulfide (CuS) nanorods were successfully synthesized.
- A facile sol–gel method without using template and complicated treatment was used.
- The as-prepared CuS nanorods as anode achieve great electrochemical performance.

ARTICLE INFO

Keywords:
Copper sulphide
Nanorods
Long-cycle life
Anode
Lithium-ion batteries

ABSTRACT

Copper sulfide (CuS) nanorods with the size of sub-10 nm are synthesized via a facile sol–gel method without post–thermal treatment. The as-prepared CuS nanorods are characterized by X-ray diffraction, transmission electron microscope, and energy dispersive X-ray spectroscopy as hexagonal covellite CuS. The as-prepared CuS nanorods utilized as anode material exhibit a high reversible capacity and excellent cycling stability up to 250 cycles, as well as high Coulombic efficiency. The unique structure of the CuS nanorods should be responsible for their excellent electrochemical performance.

1. Introduction

Li-ion battery batteries have been applied in a variety of portable electronic devices and are being pursued as power sources for hybrid electric vehicles and electric vehicles [1,2]. Commercially available Li-ion batteries utilize an intercalation-based graphite anode coupled with a lithium-transition metal oxide or phosphate cathode. The graphite anode with a theoretical capacity of 372 mAh g^{-1} cannot enable the creation of batteries that achieve the high energy density required for vehicles and other emerging applications, which has motivated research into new high-capacity anode materials. A significant advance in the field comes with the discovery of materials that operate via a conversion reaction. 3d-transition metal compounds M_xX_y (M = Co, Fe, Ni, Cu, etc.; X = F, O, S, N, etc.) based on the conversion reaction have now been widely investigated for their potential use in Li-ion batteries because of their high capacities [3]. In these materials, transition metal sulfides, such as ZnS, CuS and MoS_2, have been widely studied during the past few decades because of their unusual physicochemical properties [4–7]. In particular, copper sulfides including CuS, $Cu_{1.75}S$, $Cu_{1.8}S$, $Cu_{1.95}S$ and Cu_2S are of great interest with potential applications ranging from energy storage, owing to their variations in stoichiometric compositions, complex structures, nanocrystalline morphologies, and valence states [7–10]. Among them, covellite CuS with a high electrical conductivity (10^{-3} S cm^{-1}) and a high theoretical capacity (560 mAh g^{-1}) with flat discharge curves

* Corresponding author. Tel./fax: +86 574 86324027.
** Corresponding author. Tel./fax: +86 574 86324027.
E-mail addresses: xiayg@nimte.ac.cn (Y. Xia), liuzp@nimte.ac.cn (Z. Liu).

when cycled versus Li^+/Li, has been studied as cathode material for Li-ion batteries [11–13]. However, the challenge of CuS used as electrodes in Li-ion batteries is the rapid drop in capacity and the formation of lithium polysulfides, which dissolve into electrolyte and drift away from the electrode. Hence, the cycle stability is a key issue for CuS used as an electrode material in Li-ion batteries. To overcome the issue, many attempts have focused on the synthesis of various nanostructures of CuS, including flowers [14–16], complex hierarchical nanostructure [17–22], one-dimensional nanostructure [23–25]. All these nanoscale morphologies somewhat improves the electrochemical performance of CuS electrodes due to their nanostructure, which can increase reaction sites, short the path of ion motion, and improve efficient charge transport. However, the preparation techniques involved mostly template-based, surfactant-directed, or interface methods. These growth methods usually require the use of special instruments, surfactants, or templates, which will increase the difficulty of operation, the cost, and contamination. In the present work, uniform small sized of sub-10 nm CuS rods were prepared via a facile sol–gel method without using template and complicated post-treatment. This method utilizes low temperature, no protective gas and cheap chemicals that make our method advantageous. Meanwhile, the electrochemical properties of as-prepared CuS nanorods as an anode material were investigated for Li-ion batteries.

2. Experimental

2.1. Chemicals

Copper acetate monohydrate (analytical reagent (AR)), pyridine (AR), and sodium sulfide nonahydrate (AR) were purchased from Sigma–Aldrich. The electrolyte was purchased from Guo Tai Hua Long Company, including 1 M $LiPF_6$ in ethylene carbonate (EC) and dimethyl carbonate (DMC) (1:1 by volume). All chemicals were used without further purification.

2.2. Synthesis of the CuS nanorods

In a typical synthesis, 5.0 mmol of copper acetate monohydrate was dissolved into 40 mL distilled water/pyridine mixture (v:v = 1:3) and heated to 80 °C. 5.0 mmol of sodium sulfide nonahydrate was dissolved into 20 mL of distilled water. Then, sodium sulfide solution was dropped into copper acetate solution under vigorous stirring. Finally, the mixture reacted for 2 h at 80 °C. The final products was collected and washed several times by distilled water or other solvents (e.g., ethanol, pyridine), and then dried in a vacuum at 60 °C for 12 h.

2.3. Material characterization

The phase composition of the as-prepared CuS samples was characterized by using a Bruker D8 Advance diffractometer (XRD) with Cu Kα radiation, at 2θ range of 20°–70° with 0.02 per step. The morphology and size of CuS nanorods were determined by FEI Tecnai F20 transmission electron microscope (TEM) coupled with energy dispersive X-ray spectroscopy (EDX). Raman spectra were measured using a Renishaw in Via-reflex spectrometer with the 532 nm line of the Ar ion laser as an excitation source in a quasi-backscattering configuration.

2.4. Electrochemical measurement

The as-prepared CuS nanorods were studied as anode materials for Li-ion batteries. The CuS electrodes were prepared by dispersing 70 wt.% active materials, 20 wt.% conductive carbon, and 10 wt.% poly(vinylidenefluride) (PVDF) binder in 1-methyl-2-pyrrolidinone (NMP) to stir for 4 h to form a homogeneous slurry. The slurry was coated onto copper foil, dried at 100 °C in a vacuum oven for 12 h, and cut into 1/2 in. diameter electrodes for testing. The amount of material on the Cu foil was in the range of 1–2 mg, thus the active material loading was calculated to be ca. 0.7–1.4 mg. Li foils and polypropylene films were used as counter electrodes and separators, respectively. The electrolyte was 1 M $LiPF_6$ in a mixture of ethylene carbonate (EC) and dimethyl carbonate (DMC) (1:1 by volume). The galvanostatic charge and discharge tests were carried out at a constant current between 0.01 and 3.0 V using a battery tester. Cyclic voltammetry (CV) was performed at a scan rate of 0.1 mV s^{-1} within the range of 0.01–3 V using an Autolab PGSTAT302N (Metrohm, Switzerland). Electrochemical impedance spectroscopy (EIS) measurements were collected by an Autolab83710 impedance analyzer, using an alternating current with an amplitude voltage of 5 mV in the frequency range of 0.1–100 KHz to CuS electrodes before and after 3 cycles.

3. Results and discussion

Fig. 1 shows the XRD pattern of the as-prepared CuS nanorods. All diffraction peaks can be indexed to the hexagonal covellite CuS structure, and no impurity phase can be detected, indicating the formation of pure CuS. The sharp diffraction peaks suggest that the obtained CuS particles were highly crystalline. To be emphasized, the disappearance of the (107) diffraction peak from the XRD pattern indicated preferentially orientation effects of the growth direction along the (110) plane of hexagonal CuS [26]. The broadening of the diffraction peaks also indicates that the products have small size.

Fig. 2 shows TEM images of the as-prepared CuS at a high magnification, together with the corresponding scanning EDX analysis. The Raman spectrum of CuS is also plotted in Fig. 2. The CuS particles were irregularly shaped in rods with size less than 10 nm and aggregated together, as shown in Fig. 2a. A high-resolution transmission electron (HR-TEM) image (Fig. 2b) clearly shows that the particle was single crystal with clear interplanar distances of 0.28 nm, corresponding to that of the (103) plane of the hexagonal covellite CuS. EDX analysis (Fig. 2c) reveals that copper and sulfur elements were detected and their atomic ratio was close to 1:1, which agrees with the stoichiometric ratio of CuS. Raman spectroscopy was employed to further characterize the overall symmetry of the as-prepared CuS nanorods, as shown in Fig. 2d. A

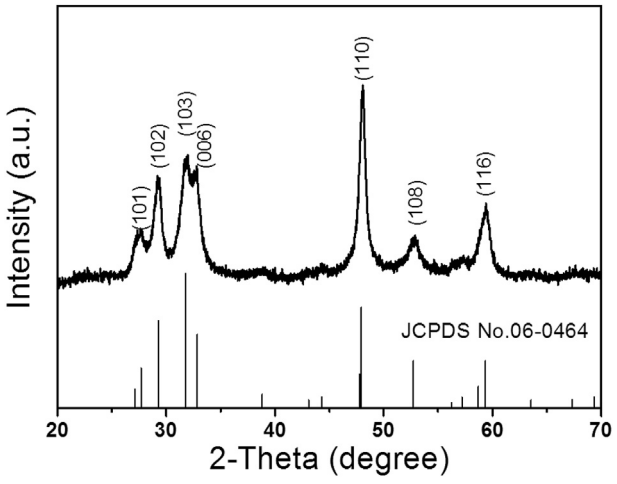

Fig. 1. The X-ray diffraction (XRD) patterns of as-prepared CuS nanorods.

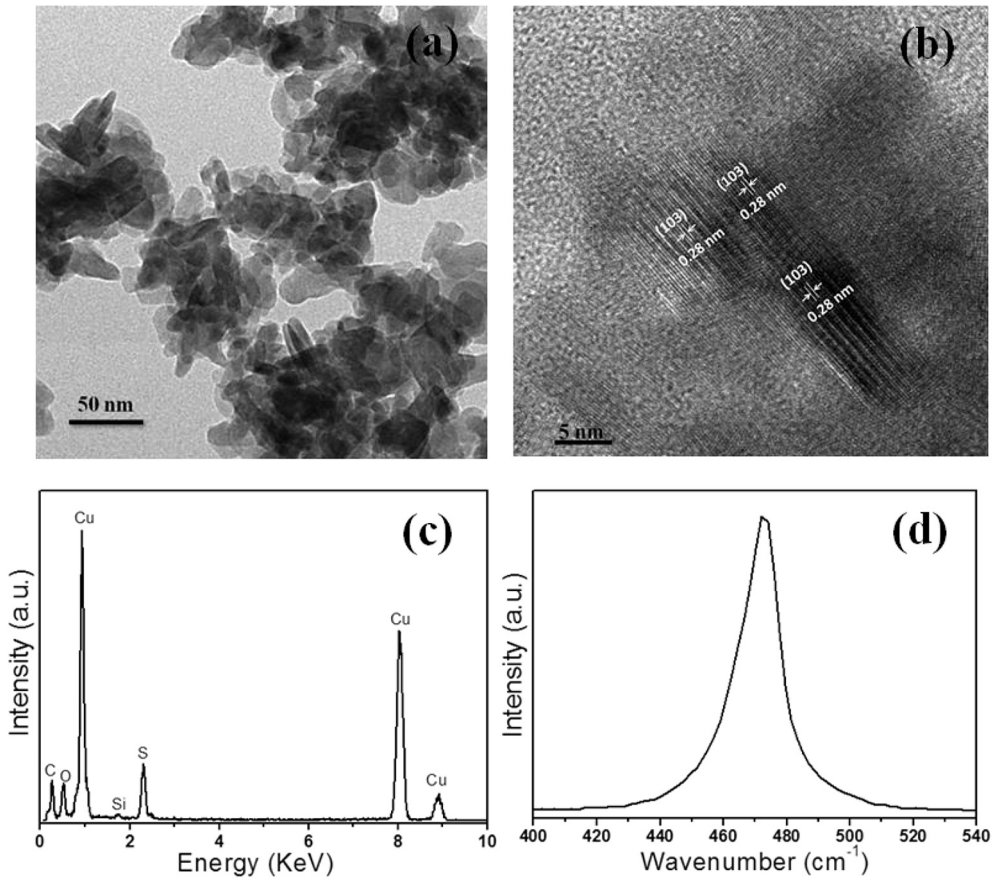

Fig. 2. (a) TEM image of CuS nanorods. (b) HRTEM image of CuS nanorods. (c) EDX elemental analysis of CuS nanorods. (d) Raman spectrum of CuS nanorods.

distinct peak wavenumber around 467 cm^{-1} is ascribed to S–S stretching vibrational mode of the covellite system [27].

The electrochemical properties of the as-prepared CuS nanorods as an anode material in 1 M $LiPF_6$/EC + DMC electrolyte are shown in Fig. 3. Fig. 3a shows the charge–discharge profiles of the CuS electrode for the first, second, third, tenth, fiftieth, and hundredth cycle at a constant current rate of 0.2 C (1C = 560 mAh g^{-1}). The initial discharge and charge capacities were 775 and 561 mAh g^{-1}, respectively. The initial discharge capacity was larger than the theoretical capacity (560 mAh g^{-1}) due to the formation of a solid electrolyte interphase (SEI), which was also reported in previous literatures [28,29]. After the second cycle, the charge and discharge reaction proceeded reversibly and the irreversible capacity was small, although the discharge capacity decreased slowly. It can be seen from Fig. 3a that the charge/discharge reaction process consisted of two main steps. During the discharge process, a slope plateau at around 2.1 V was observed, and the second plateau was found at about 1.7 V, followed by a long slope until cutoff voltage (0.01 V). However, these two plateaus became shorter and shifted to higher voltages of 1.9 and 2.4 V, respectively, during the charge process. To verify the electrochemical reactions, CV measurements were preformed with Li metal as the counter electrode in the voltage range of 0.01–3 V at the scan rate of 0.1 mV s^{-1} (Fig. 3b). Two pair of distinct redox current peaks can be clearly observed from the CV curves. Similar results have been reported for CuS electrode in previous literatures [30]. During the first cycle, the oxidation peaks were located at ~1.9 and ~2.4 V, whereas the corresponding reduction peaks were observed at ~2.1 and ~1.7 V. These indicated that discharging reactions occurred at around 1.9 and 2.4 V and that peaks for the charging reactions appeared at around 2.1 and 1.7 V, which coincides with the discharge–charge curves in Fig. 3a. From the second cycle, all the peaks decreased gradually, especially for the oxidation peak at around 2.4 V and the reduction peak at round 2.1 V, corresponding to the plateau changes between the 1st and 2nd cycle (Fig. 3a). Furthermore, two reduction peaks occurred at about 2.1 and 1.7 V were attributed to lithiation of CuS and Li_xCuS, respectively, while the oxidation peaks at 1.9 and 2.4 V were attributed to reverse reactions [10].

Fig. 3c shows the cycling performance of CuS electrodes at a constant current of 0.2 C (1C = 560 mA g^{-1}). As shown in Fig. 3c, the capacity of CuS nanorods decreased gradually in the first 10 cycles, and then stabilized at ~390 mAh g^{-1} with a small fluctuation up to 250 cycles. Furthermore, this novel CuS anode showed an initial Coulombic efficiency of 69.8%, which increased to ~90.1% at the second cycle, and further increased to ~97.2% at the 10th cycle, and finally stabilized at ~99.1% in subsequent cycles. To the best of our knowledge, it demonstrates a much longer cycle life than that previously reported for CuS electrode, indicated that the CuS nanorods can be a promising electrode material for Li-ion batteries.

In additional to high capacity and excellent cyclability, the CuS nanorods also exhibit a good rate capability, as shown in Fig. 3d. The rate capability of CuS nanorods was studied using the galvanostatic charge/discharge tests. The current rate increased from 0.1 C to 5.0 C, seven cycles were recorded for each stepwise increment. When the current density was 0.1 C, the CuS anode showed a reversible capacity of ~400 mAh g^{-1}. Although the capacity gradually decreased while the current rate increased from 0.1 C to 5.0 C, the CuS electrode still has a capacity of ~182 mAh g^{-1} at a high current rate of 5.0 C. Moreover, when the rate returned to the initial 0.1 C, the CuS electrode recovered its capacity of ~410 mAh g^{-1}. The

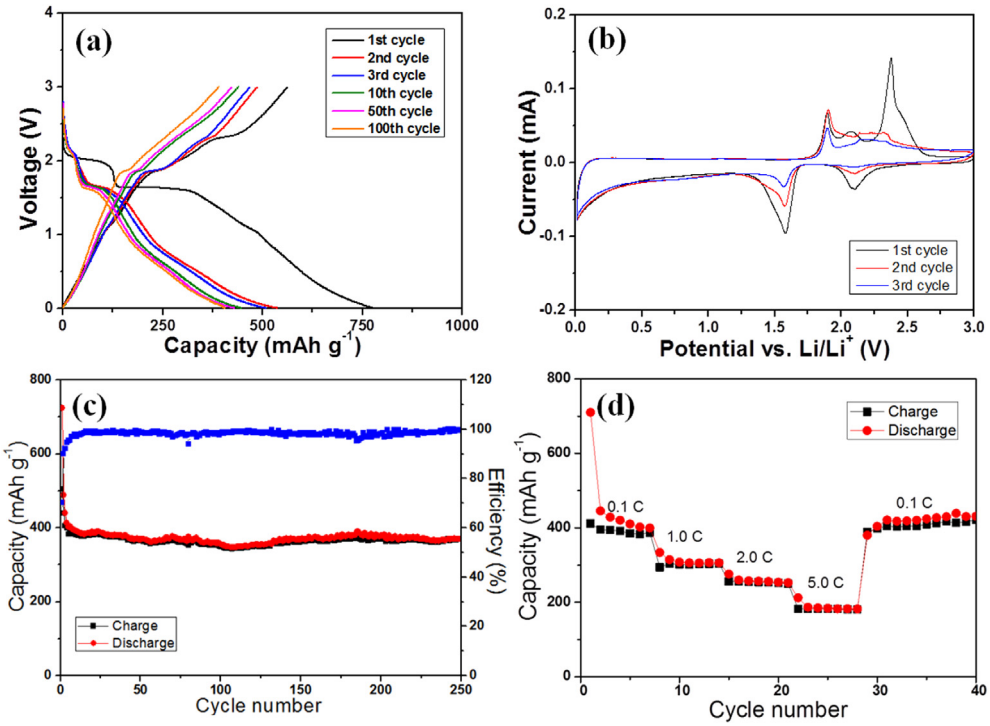

Fig. 3. (a) Charge and discharge curves of CuS nanorods as anode. (b) CV curves of CuS electrodes in the half cells cycled between 0.01 and 3.0 V (vs. Li^+/Li) at a rate of 0.1 mV s^{-1}. (c) Cycling performance of CuS electrodes at 0.2 C. (d) Galvanostatic rate capability of CuS electrodes.

long-cycle life and high rate performance of CuS nanorods were strongly related to the advantages as following: (1) the unique structure of sub-10 nm nanorods can provide effective accommodation of the strain during cycling, shorten the path of ion motion, enhance efficient charge transport, and accelerate the rate of chemical and energy transformation processes; (2) the intrinsic characteristic of CuS with good electronic conductivity can significantly improve its performance [30,31].

EIS was carried out to compare the CuS samples as the working electrodes *versus* Li before and after 3 cycles. Fig. 4 shows Nyquist plots of the CuS cells before and after 3 cycles. It was apparently seen that the impedance spectrum is composed of a semicircle at high-to-medium frequency region, and a straight sloping line at low frequency region. Similar large semicircles in both cases indicated that both have a similar charge transfer resistance (R_{ct}, relating the charge transfer through the electrode/electrolyte interface) of CuS. This phenomenon can support the superior performance in Li-ion batteries, especially for the excellent cyclability (Fig. 3). However, the slope of lines at low frequency region, which corresponds to Warburg impedance (Z_w, relating to the diffusion of lithium ions in the electrode), was different before and after cycling. For the change of the slope before and after cycling, the main reason could be rooted in the conversion reaction of CuS nanorods after lithiation and delithiation, resulting in the bulk structural rearrangement that greatly differs from the pristine one. Therefore, the changed slope that corresponds to Warburg impedance is reasonable.

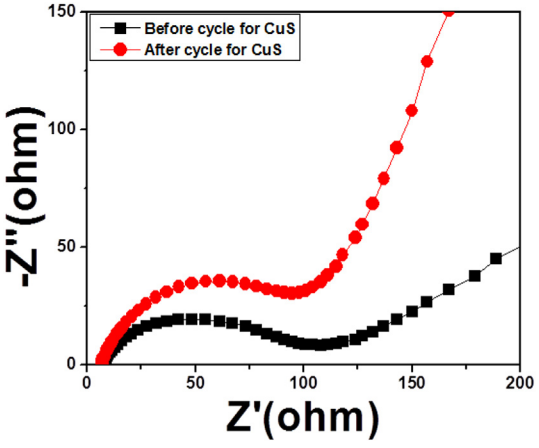

Fig. 4. Nyquist plots of Li-ion cells using CuS electrodes before and after 3 cycles.

4. Conclusion

In summary, we developed a facile solution approach to fabricate CuS nanorods with the size less than 10 nm. Our method which used cheap chemicals and processed in low temperature without protective gas was promising for mass production. The as-prepared CuS nanorods were used as anode materials exhibited excellent electrochemical performance in Li-ion batteries. The unique structure of CuS nanorods should be responsible for the enhanced performance, including high reversible capacity, high coulombic efficiency, great capacity retention, and superior rate capability. Herein, the CuS nanorods can be a promising electrode material for Li-ion batteries.

Acknowledgment

This work was financially supported by Scientific Research Foundation for Startup Researcher (ZX2013000556), Natural Science Foundation of Ningbo (ZX2014000631), Education Foundation of Zhejiang Province (ZX2014000283). This work was also sponsored by K.C. Wong Magna Fund in Ningbo University.

References

[1] M. Zhou, L. Zhao, T. Doi, S. Okada, J. Yamaki, J. Power Sources 195 (2010) 4952–4956.
[2] M. Zhou, M. Gordin, S. Chen, T. Xu, J. Song, D. Lv, D. Wang, Electrochem. Commun. 28 (2013) 79–82.
[3] N. Yamakawa, M. Jiang, C.P. Grey, Chem. Mater 21 (2009) 3162–3176.
[4] X. Chen, H. Xu, N. Xu, F. Zhao, W. Lin, G. Lin, Y. Fu, Z. Huang, H. Wang, M. Wu, Inorg. Chem. 42 (2003) 3100–3106.
[5] C. Wu, S. Yu, S. Chen, G. Liu, B. Liu, J. Mater. Chem. 16 (2006) 3326–3331.
[6] J. Tang, A.P. Alivisators, Nano Lett. 6 (2006) 2701–2706.
[7] Y. Chen, C. Davosine, J.M. Tarascon, C. Guery, J. Chem. Mater 22 (2012) 5295–5299.
[8] X. Jiang, Y. Xie, J. Lu, W. He, L. Zhu, Y. Qian, J. Mater. Chem. 10 (2000) 2193–2196.
[9] P. Kumar, R. Nagarajan, Inorg. Chem. 50 (2011) 9204–9206.
[10] X. Wang, Y. Wang, X. Li, B. Liu, J. Zhao, J. Power Sources 281 (2015) 185–191.
[11] K. Okamoto, S. Kawai, Jpn. J. Appl. Phys. 12 (1973) 1130–1138.
[12] A. Etienne, J. Electrochem. Soc. 117 (1970) 870–874.
[13] J.S. Chung, H.J. Sohn, J. Power Sources 108 (2002) 226–231.
[14] J. Gao, Q. Li, H. Zhao, L. Li, C. Liu, Q. Gong, L. Qi, Chem. Mater 20 (2008) 6263–6269.
[15] Li Zhao, F. Tao, Z. Quan, X. Zhou, Y. Yuan, J. Hu, Mater. Lett. 68 (2012) 28–31.
[16] M. Nagarathinam, K. Saravanan, W. Leong, P. Balaya, J. Vittal, Cryst. Growth Des. 9 (2009) 4461–4470.
[17] H. Yan, W. Wang, H. Xu, J. Cryst. Growth 310 (2008) 2640–2643.
[18] C. Mu, Q. Yao, X. Qu, G. Zhou, M. Li, S. Fu, Colloids Surf. A 371 (2010) 14–21.
[19] Y. Chen, C. Davoisne, J. Tarascon, C. Gu ery, J. Mater. Chem. 22 (2012) 5295–5299.
[20] Y. Han, Y. Wang, W. Gao, Y. Wang, L. Jiao, H. Yuan, S. Liu, Powder Technol. 212 (2011) 64–68.
[21] J. Kundu, D. Pradhan, New. J. Chem. 37 (2013) 1470–1478.
[22] S. Yang, H. Yao, M. Gao, S. Yu, CrystEngComm 11 (2009) 1383–1390.
[23] C. Wu, J. Shi, C. Chen, Y. Chen, Y. Lin, P. Wu, S. Wei, Mater. Lett. 62 (2008) 1074–1077.
[24] P. Roy, K. Mondal, S. Srivastava, Cryst. Growth. Des. 8 (2008) 1530–1534.
[25] C. Wu, S. Yu, S. Chen, G. Liu, B. Liu, J. Mater. Chem. 16 (2006) 3326–3331.
[26] Y. Ni, H. Liu, F. Wang, G. Yin, J. Hong, X. Ma, Z. Xu, J. Appl. Phys. A 10 (2003) 332–335.
[27] B.M. Sukarawa, M. Najdoski, I. Grozdanov, C.J. Chunnial, J. Mol. Struct. 267 (1997) 410–411.
[28] Q. Li, Y. Xue, Y. Zhu, Y. Qian, J. Nanosci. Nanotechnol. 13 (2013) 1265–1269.
[29] Y. Gu, Y. Xu, Y. Wang, ACS Appl. Mater. Interfaces 5 (2013) 801–806.
[30] C. Feng, L. Zhang, Z. Wang, X. Song, K. Sun, F. Xu, G. Liu, J. Power Sources 269 (2014) 550–555.
[31] C. Lai, K. Huang, J. Cheng, C. Lee, W. Lee, W. Lee, C. Huang, B. Hwang, L. Chen, J. Mater. Chem. 19 (2009) 7277–7283.